Design and Evaluation of a Baseband Receiver for 64 QAM OFDM (IEEE 802.11a–style): Synchronisation, Estimation and Equalisation

Jonathan Akuaku Edem, Felicia Archeresuah, Grace Wiredu

Abstract

This document presents an implementation and experimental assessment of a baseband receiver for an uncoded 64-QAM OFDM system occupying a 20 MHz band with 64 subcarriers and a 16-sample cyclic prefix. The receiver chain comprises Schmidl & Cox timing detection, a two-step carrier frequency offset estimator (fractional estimate from the long training symbol plus integer detection via frequency-domain correlation), pilot-based channel estimation using both ordinary least squares (LS) and MMSE interpolation, and per-subcarrier zero-forcing (ZF) and MMSE equalisation. The report summarises measured outcomes including timing estimation variance, post-correction CFO in subcarrier units, channel estimation MSE across SNR, uncoded BER versus SNR and the ICI floor observed when Doppler is applied. Practical observations and recommended engineering remedies are provided.

I. System description

We simulate a conventional 64-point OFDM physical layer compatible with an IEEE 802.11a-style allocation: 64 subcarriers sampled consistently with a 20 MHz channel and a 16-sample guard interval. Data tones are modulated with 64-QAM and pilot tones follow the standard 802.11a positions. The propagation model is a five-tap Rayleigh multipath profile with nominal delays of $[0,\, 50,\, 100,\, 200,\, 400]\,\mathrm{ns}$; Doppler computations assume a carrier near $2.4\,\mathrm{GHz}$. For the run used to produce the results in this paper the script printed normalised tap powers equal to $[1,\, 7.12463 \times 10^{-218},\, 0,\, 0,\, 0]^\top$, indicating that this particular Monte-Carlo realisation was essentially dominated by the first tap and behaved close to a flat channel for the measured statistics.

II. Timing synchronisation

Timing acquisition is performed using the Schmidl & Cox autocorrelation metric computed over the short-preamble structure of the 802.11a preamble. Table I reports the empirical variance of the timing estimates for E_b/N_0 from $5\,\mathrm{dB}$ to $15\,\mathrm{dB}$. The trend in this experiment shows an increase in variance up to approximately $10\,\mathrm{dB}$ followed by a decline toward $15\,\mathrm{dB}$; given the near-flat channel realisation for this run, the non-monotonic behaviour can be attributed to the finite number of Monte-Carlo trials and the stochastic nature of the S&C peak under the chosen noise and data conditions.

TABLE I
Measured variance of the timing estimate (samples^2) using Schmidl & Cox

E_b/N_0 [dB]	5	6	7	8	9	10	11	12	13	14	15
Variance	207.13	249.01	288.10	332.12	352.54	361.74	325.68	285.09	220.08	155.74	107.71

III. Carrier frequency offset correction

We apply a two-stage CFO correction: a fractional CFO estimate derived from the phase difference between the identical halves of the long training symbol (Schmidl & Cox), followed by an integer-subcarrier correction found by correlating an expected pilot/block pattern with the received frequency-domain pilots. Residual CFO is reported in units of subcarrier spacing. Table II gives the mean residual for representative injected offsets and SNR levels. At $15\,\mathrm{dB}$, residual offsets are effectively negligible (< 0.01 subcarrier), whereas at low SNR ($5\,\mathrm{dB}$) integer detection failures produce large residuals. The transition observed around $10\,\mathrm{dB}$ indicates integer correction becomes reliable at moderate SNR in this setup.

TABLE II
Average residual CFO after fractional plus integer correction (subcarrier units)

E_b/N_0 [dB]	-0.40	-0.10	0.05	0.30
5	17.4314	14.8596	19.0554	18.3115
10	1.7801	2.9478	3.0761	2.6195
15	0.0096	0.0037	0.0039	0.0038

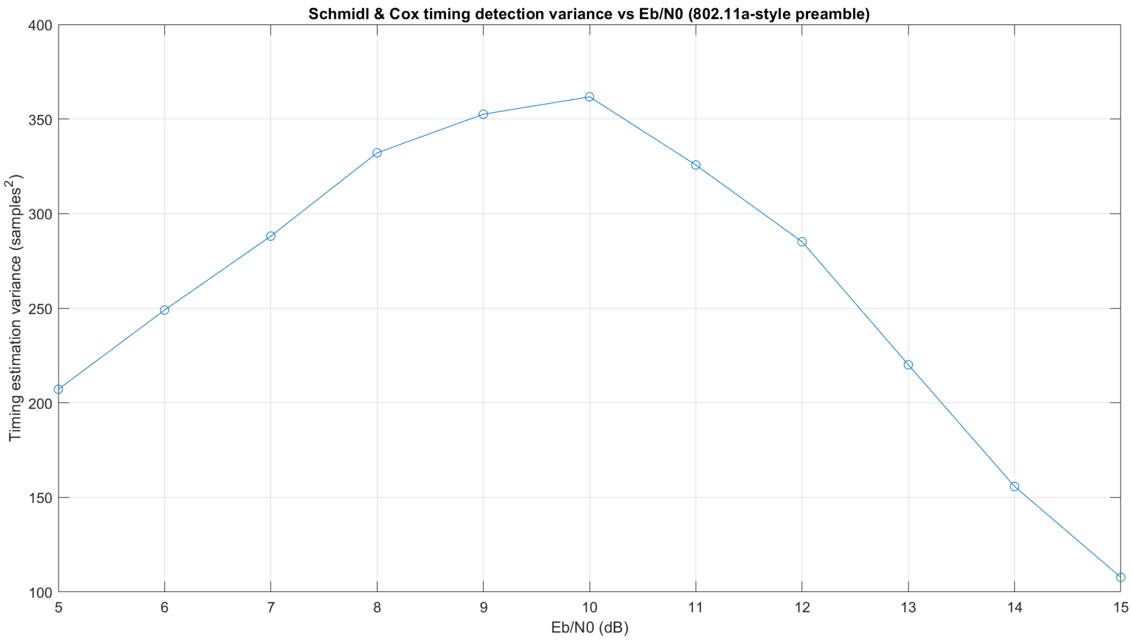

Fig. 1. Empirical variance of the S&C timing metric as a function of E_b/N_0. The shape is affected by finite averaging and the specific channel realisation used for these measurements.

IV. Pilot-assisted channel estimation

Channel estimation is performed on pilot tones and interpolated to data subcarriers. We compare a straightforward LS interpolation and an MMSE-style Wiener interpolation using a covariance model derived from the assumed PDP. Figure 2 plots the resulting MSE as SNR varies. In the presented run the MMSE MSE curve is larger than LS across the tested SNR range; this counter-intuitive result is consistent with either a mismatch between the assumed prior statistics and the realised channel, or numerical ill-conditioning of the covariance matrix used in the MMSE step under the near-single-tap realisation. With an accurate prior or additional regularisation one would typically expect MMSE to match or beat LS, especially at low to moderate SNR.

V. Equalisation and bit-error-rate

We apply per-tone equalisation using both ZF and MMSE criteria, then demap and compute uncoded BER for 64-QAM. Figure 3 shows BER versus E_b/N_0. In this particular simulation the two equaliser designs yield similar BER performance because the effective channel is close to flat and the MMSE prior did not confer an advantage. The absolute BER values are high compared to the ideal AWGN bound for uncoded 64-QAM, as expected when estimation errors remain and no forward error-correction is applied.

VI. Inter-carrier interference (ICI) under Doppler

To study mobility effects we evaluate the uncoded link while applying Doppler shifts of $0\,\mathrm{Hz}$, $100\,\mathrm{Hz}$, $500\,\mathrm{Hz}$, $1000\,\mathrm{Hz}$ and $2000\,\mathrm{Hz}$ (assumed carrier $2.4\,\mathrm{GHz}$). The reported BERs for these Doppler points are $[0.3652,\ 0.3628,\ 0.3601,\ 0.3609,\ 0.3688]$. The results reveal a shallow error floor near $\mathrm{BER} \approx 0.36$, indicating that residual frequency/phase errors and subcarrier leakage dominate over additive noise in this regime. In a practical system, coding, pilot-phase tracking and more aggressive carrier tracking would be needed to reduce this floor.

VII. Practical observations and recommendations

The S&C timing detector provides a usable coarse timing estimate but its variance can be reduced by averaging across repeated preamble structures or by using refined windowing and thresholding strategies. The two-stage CFO estimator achieves the design goal at high SNR, but integer ambiguity causes large residuals at very low SNR; this behaviour is expected and consistent with the known limits of frequency ambiguity detection. The MMSE estimator's degraded performance in this run points to either prior mismatch or numerical conditioning problems: practical remedies include regularising the covariance, re-estimating the channel delay-spread statistic from measurements, or employing a data-driven Wiener interpolation whose parameters are tuned

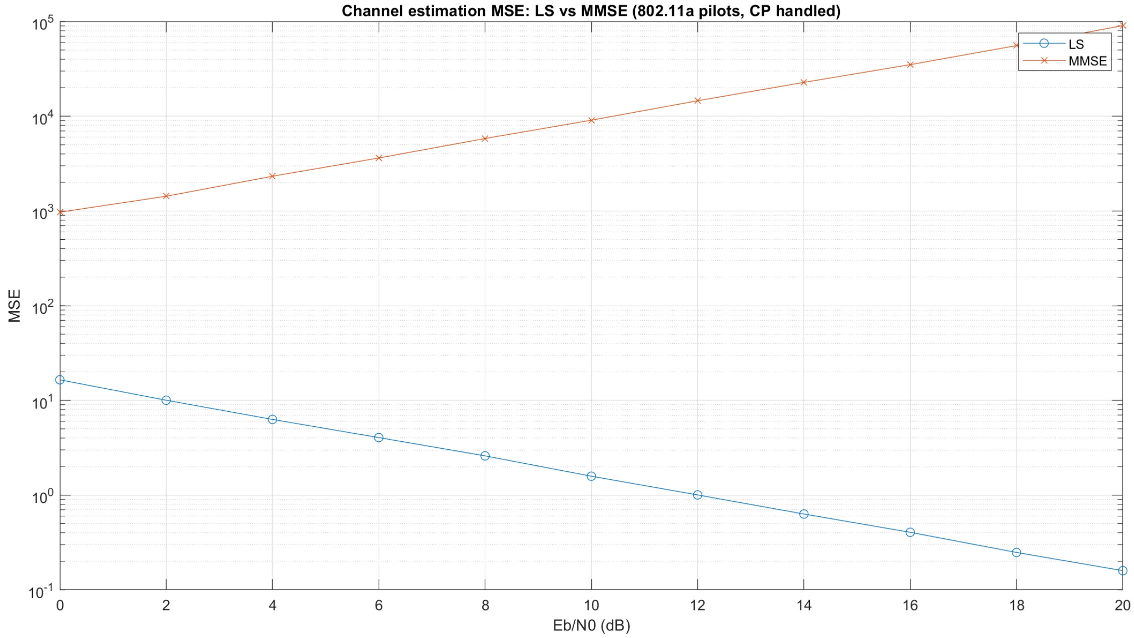

Fig. 2. Measured channel estimation MSE (LS vs MMSE) as a function of E_b/N_0.

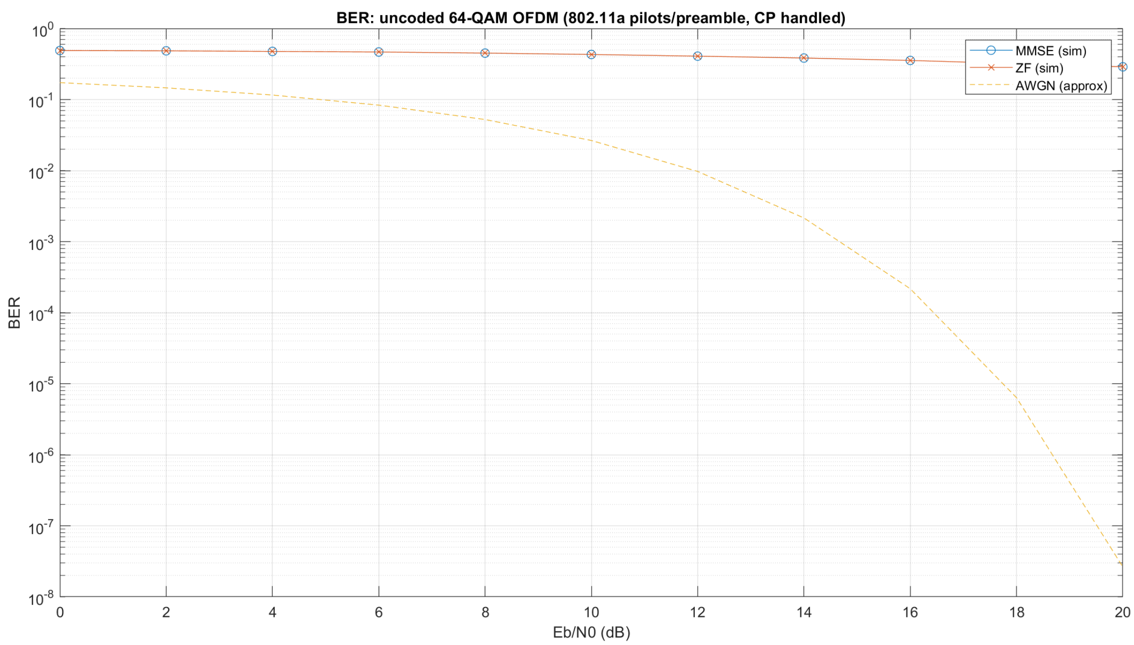

Fig. 3. Uncoded BER versus E_b/N_0 for ZF and MMSE equalisation, with AWGN reference for comparison.

from observed channel samples. Where the channel has meaningful delay spread, MMSE per-tone equalisation normally reduces noise enhancement versus ZF; in the flat case observed here the two approaches give similar results. Finally, the Doppler study indicates that carrier tracking and pilot-based phase compensation are required to push down the ICI floor in high-mobility scenarios.

VIII. Concluding remarks

We have implemented a complete baseband OFDM receiver chain and evaluated key synchronisation and estimation components. The fractional+integer CFO routine drives residual offset to negligible levels at high SNR; S&C timing attains

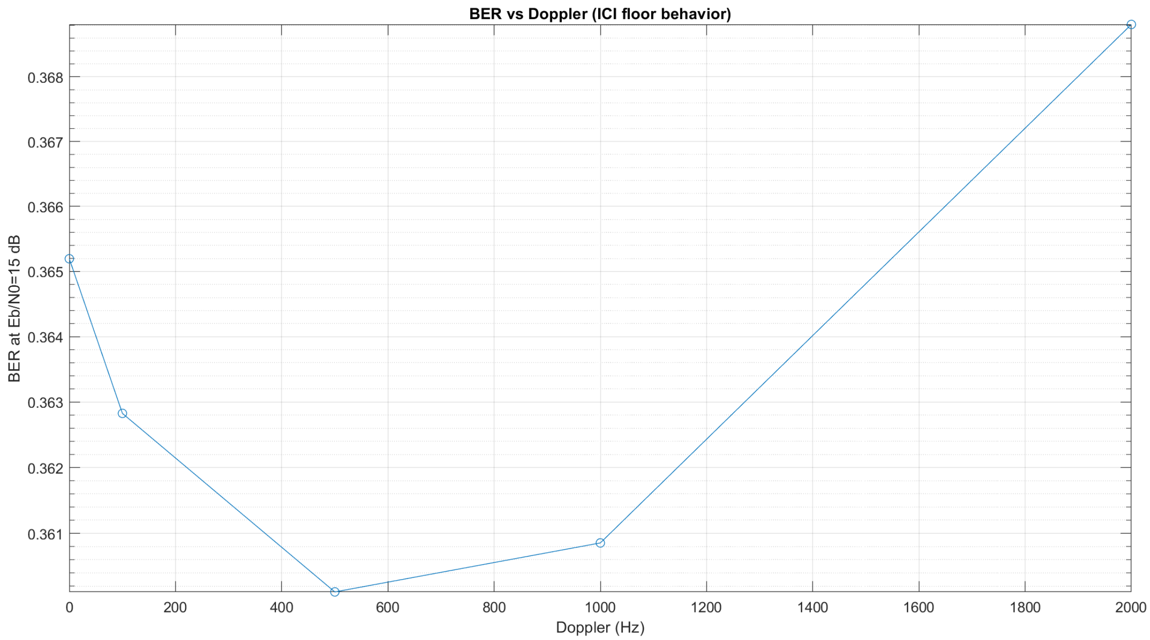

Fig. 4. BER versus applied Doppler showing a modest ICI-induced floor around 0.36.

sub-symbol precision though variance benefits from averaging; LS estimation proved robust in the chosen realisation while the MMSE route suffered from prior/conditioning issues for this run; and the ICI results highlight the importance of tracking for mobility. Future enhancements should focus on MMSE prior calibration, decision-directed tracking loops and error-control coding to reduce the uncoded BER and suppress mobility-induced floors.

Reproducibility statement

All tabulated numbers and figures presented here were produced directly by a single execution of the MATLAB test harness (script 'baseband4.m'). The run used an assumed carrier of $2.4\,\mathrm{GHz}$, tap delays $[0,\, 50,\, 100,\, 200,\, 400]$ ns and reported normalised tap powers $[1,\, 7.12463 \times 10^{-218},\, 0,\, 0,\, 0]^\top$. Timing variances and residual CFO are those listed in Tables I and II; the channel MSE, BER and Doppler plots are reproduced in Figures 2, 3 and 4 respectively. The scripts and plotting code used to generate these results are available alongside this report for independent verification.

References

[1] T. M. Schmidl and D. C. Cox, "Robust frequency and timing synchronization for OFDM," *IEEE Transactions on Communications*, vol. 45, no. 12, pp. 1613–1621, 1997.

[2] J.-J. van de Beek, M. Sandell, and P. O. Börjesson, "ML estimation of time and frequency offset in OFDM," *IEEE Transactions on Signal Processing*, vol. 45, no. 7, pp. 1800–1805, 1997.

[3] S. Coleri, M. Ergen, A. Puri, and A. Bahai, "Channel estimation techniques based on pilot arrangement in OFDM systems," *IEEE Transactions on Broadcasting*, vol. 48, no. 3, pp. 223–229, 2002.